35th Annual International Conference of the IEEE EMBS
Osaka, Japan, 3 - 7 July, 2013

Aortic Valve Segmentation from Ultrasound Images Based on Shape Constraint CV Model

Bin Dong, Yiting Guo, Bing Wang, Lixu Gu*

Abstract— **Image Guided Intervention for valvular heart disease is increasingly making progress in minimally invasive manner, where effective and accurate segmentation of aortic valve (AV) from echocardiography is fundamental to improve the intra operative location accuracy. This paper proposes a shape constraint Chan-Vese (CV) model for segmenting the AV from ultrasound (US) images. Considering the poor quality and speckle noise in AV US images, the problem of the overflow at the weak edge is solved by adding the shape constraint to the CV model. The predefined shape constructed from AV region is applied as an energy constraint to the energy function through a signed distance map, and the AV is detected from the US image by minimizing the energy function. A hundred AV segmentation results are analyzed in the experiment, where the evaluation parameters are 95.38±2.7%, 1.4±0.5 mm, 2.07±1.3 mm in transthoracic AV and 97.21±1.6%, 0.7±0.15 mm, 1.04±0.6 mm in transesophageal AV, which reveal that the shape constraint CV model can segment AV accurately, efficiently and robustly.**

I. Introduction

Valvular heart disease is a significant and increasing global problem which damages human health [1]. As a one-way valve, the AV controls the blood flow between the heart and the aorta, where aortic insufficiency or aortic stenosis impairs blood circulation. In clinical diagnosis, echocardiography is routinely used for observing the shape and movement of the AV, where the accurate segmentation of the AV from US image plays a crucial role in computer-aided diagnoses of cardiac disease and AV intervention operation.

The existence of various artifacts such as shadows, speckle, and signal dropouts make the segmentation task complex, where the orientation dependence of acquisition can lead to missing boundaries [2]. Methods based on a single threshold are insufficient for segmenting US images with grey information. Researchers have been trying to find solutions for more accurately segmenting US images.

With a linear combination of the grey level and the local entropy, a multivariate extension of minimum cross entropy thresholding (MCE) was used to detect the contours of ovarian cysts in sonography [3].

* *corresponding authors*
Bin Dong is with the Affiliated Hospital of Hebei University , Baoding City, Hebei, 071002, China (e-mail:dbin2000@163.com).
Yiting Guo is with the Biomedical Multidisciplinary Research Center of Hebei University, 180 Wusi East Road, Baoding City, Hebei, 071002, China (e-mail:gytinggyting@163.com).
Bing Wang is with the College of Mathematics and Computer Science, Hebei University, 180 Wusi East Road, Baoding City, Hebei, 071002, China (e-mail:wangbing@hbu.edu.cn).
Lixu Gu is with the the Biomedical Multidisciplinary Research Center of Hebei University, 180 Wusi East Road, Baoding City, Hebei, 071002, China (phone:8621-62933250; fax:8621-62933250; e-mail: gulixu@sjtu.edu.cn).

Klingler et al. [4] presented a semiautomatic technique by applying mathematical morphology and traditional threshold methods to segment the endocardium in echocardiograms.

Huang and Chen [5] proposed an efficient method for automatically extracting contours of breast tumors from US images, which takes advantages of watershed segmentation and neural network classification.

Energy-based segmentation methods have also been widely applied to the US images.

In their seminal work [6], Mumford et al. proposed the well-known Mumford-Shah functional, where the problem of image segmentation is solved by providing a piecewise smooth function that optimally approximates the image.

Based on the Mumford-Shah functional, Chan et al. proposed a new model for active contours without edges to detect objects whose boundaries are not necessarily defined by gradient or with very smooth boundaries [7].

In order to solve the problem caused by objects that are partly occluded or with fuzzy and discontinuous boundary in the image, Cremers et al. presented a novel approach to integrate shape prior into level set segmentation method [8].

We found that the CV model may cause serious overflow at the weak boundary of the object when used to segment the AV in the US images. Inspired by [8], as an energy constraint, a predefined shape is applied to the energy functional of the CV model through a signed distance map. The improved AV segmentation result from US images could be achieved by minimizing the new energy functional.

II. Methodology

Fig.1 shows the flowchart of the proposed method, which consists of three main procedures for segmenting AV from US images: (1) converting video into a sequence of images and extracting the fan-shaped ROI; (2) setting predefined shape which covers the whole AV region; and (3) minimizing the shape-driven CV model to obtain the AV segmentation results. Next, we will describe in detail how to set the predefined shapes and the CV model with shape constraint.

A. Setting Predefined Shapes

The heart has a continuing rhythmic activity. During the cardiac cycle, the AV changes its own shape and movement continuously where blood is pumped out of the heart into the aorta and the valve opens and closes. As shown in Fig. 2(a), a key image selected from echocardiography which has clear

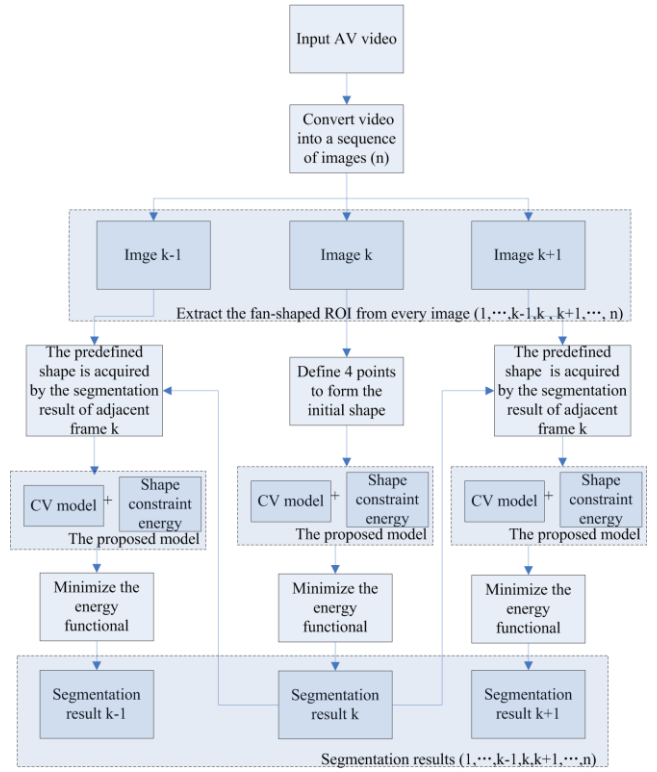

Fig.1. Flowchart of the proposed segmentation scheme

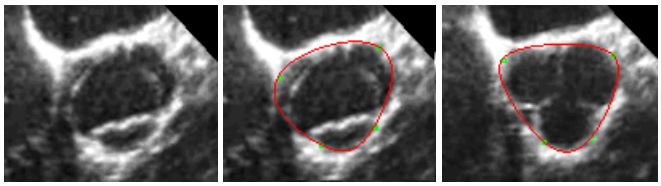

(a) (b) (c)

Fig.2. The green points are defined by users and the red closed curve is the predefined shape constructed by the cardinal spline.

boundary is determined as the image in diastolic phase where the AV is fully open. To set the initial predefined shape, as shown in Fig. 2(b) and Fig. 2(c), the user defines four points which are the slight convex points along AV borders in the key image.

The cardinal spline interpolation is employed to construct the initial predefined shape through four successive control points: P_{m-1}, P_m , P_{m+1}, and P_{m+2}. Point P_m and point P_{m+1} are the endpoints of the curve segment. The other two points are used to calculate the slope at endpoints.

For each segment curve between P_m and P_{m+1}, we have four constraint conditions:

$$\begin{aligned} P(0) &= P_m \\ P(1) &= P_{m+1} \\ P'(0) &= 0.5(1-t)(P_{m+1} - P_{m-1}) \\ P'(1) &= 0.5(1-t)(P_{m+2} - P_m) \end{aligned} \tag{1}$$

where t is a tension parameter that affects the smoothness of the curve. Since it is to be a cubic polynomial, the curve segment between these two points can be expressed as:

$$\begin{aligned} P(u) &= P_{m-1}(-su^3 + 2su^2 - su) + P_m[(2-s)u^3 + (s-3)u^2 + 1] \\ &+ P_{m+1}[(s-2)u^3 + (3-2s)u^2 + su] + P_{m+2}(su^3 - su^2) \end{aligned} \tag{2}$$

In order to reduce the interaction and to improve efficiency during the surgery, predefined shapes for other US images in Fig.1 are acquired from the segmentation results of adjacent frames.

B. The CV Model with Shape Constraint

CV model is an effective active contour segmentation model, which is suitable for the region segmentation with weak boundary. The CV energy model segments an input image $u : \Omega \to R$ by minimizing the functional which makes the active contour C approaching the boundary of the object.

$$\begin{aligned} E^{CV}(C, c_1, c_2) &= v.Area(C) + \mu.Lenghth(C) \\ &+ \lambda_1 \int_{\Omega in} |u(x,y) - c_1|^2 \, dxdy + \lambda_2 \int_{\Omega out} |u(x,y) - c_2|^2 \, dxdy \end{aligned} \tag{3}$$

where Ωin and Ωout represent the region inside and outside the contour C respectively, c_1 and c_2 are the average intensities inside and outside the contour C respectively, and $\lambda_1, \lambda_2, v, \mu$ are some positive parameters. $Area(C)$ represents the area inside the contour C. $Lenghth(C)$ calculates the length of the contour C. To facilitate the calculation, usually take v=0, $\lambda_1 = \lambda_2 = 0$ .The Euler-Lagrange equation for this energy functional with respect to ϕ can be implemented by the following gradient descent:

$$\frac{\partial \phi}{\partial t} = \delta_\varepsilon(\phi)[\mu div(\frac{\nabla \phi}{|\nabla \phi|}) - v - \lambda_1(u - c_1)^2 + \lambda_2(u - c_2)^2] = 0 \tag{4}$$

Although the method of CV model is a partial solution to the problem that the boundary of the object is unclear, there will still be overflow at the weak edge of the US image. It is essential to enlarge the image constraint force for connecting separate gaps of the object edge. To solve the overflow problem, the region-based energy constraint is added in the CV model:

$$\begin{aligned} E(\phi, c_1, c_2) &= E_{cv}(\phi, c_1, c_2) + \alpha E_{shape}(\phi) \\ &= \mu \int_\Omega \delta(\phi) |\nabla \phi| dxdy + v \int_\Omega H(\phi) dxdy \\ &+ \lambda_1 \int_\Omega |u(x,y) - c_1|^2 H(\phi) dxdy \\ &+ \lambda_2 \int_\Omega |u(x,y) - c_2|^2 (1 - H(\phi)) dxdy \\ &+ \alpha \int_\Omega (\phi - \phi_0)^2 dxdy \end{aligned} \tag{5}$$

where, α is a positive parameter which affects curve evolution with the shape-driven energy.

The gradient descent equation for ϕ is given by:

$$\begin{aligned} \frac{\partial \phi}{\partial t} &= \delta_\varepsilon(\phi)[\mu div(\frac{\nabla \phi}{|\nabla \phi|}) - v - \lambda_1(u - c_1)^2 + \lambda_2(u - c_2)^2] \\ &- 2\alpha(\phi - \phi_0) \end{aligned} \tag{6}$$

The segmentation result is then obtained by minimizing the proposed energy functional.

III. THE EXPERIMENTAL RESULTS

A. Experiment Data and Environment

The experiment focuses on the AV short axis view where the AV B-mode US data are downloaded from http://www.echobyweb.com/index.htm. The experimental data which is acquired by Philips Sonor 5500 is divided in two categories: one is transthoracic data with transducer frequency 2.5 MHz which is more blurred; the other is transesophageal data with transducer frequency 4.4 MHz which has relatively clear boundary. Most of the US instrument supports AVI format output. To obtain the sequence of the AV US images, DirectShow and FFDShow media decoder are used to convert video into a sequence of images each with 224*256 pixels.

The proposed mechanisms are implemented on a desktop PC computer with Pentium® Dual-Core CPU E5800 @ 3.20GHz, 2GB RAM, NVIDIA GeForce GT 430 GPU, with Matlab 7.11.0 and VS2008 on Windows XP.

B. Experiment Process and Parameter Estimation

The general experimental framework is shown in Fig. 3.

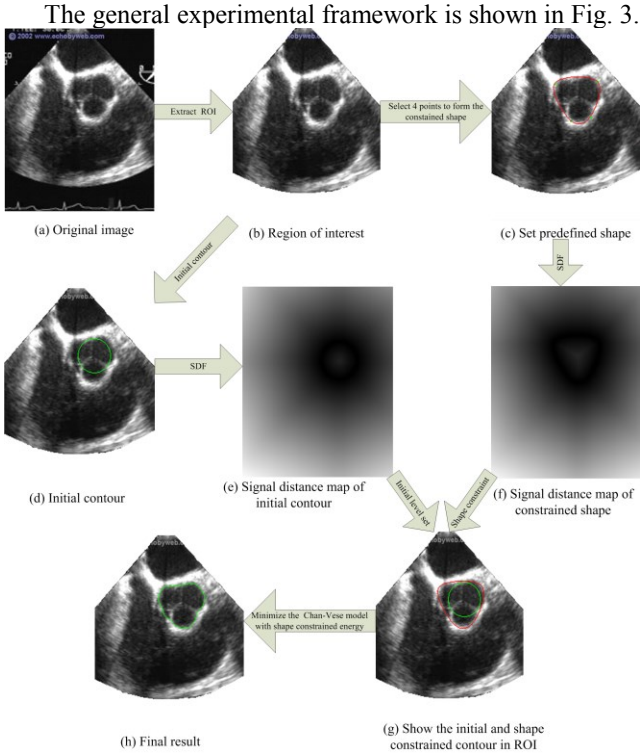

Fig. 3. An example of transesophageal AV segmentation experiment framework.

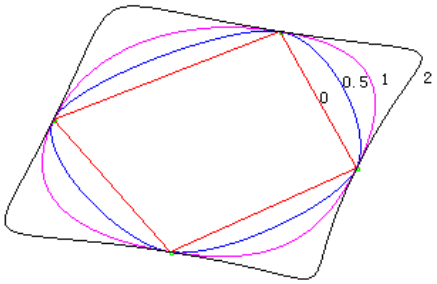

Fig. 4. The closed cardinal spline curve with different tension parameter *t*.

Two parameters need to be determined in the experiment. One is the tension parameter *t* in cardinal spline interpolation. Cardinal splines with different values of the tension parameter will produce different closed curve through four points. Fig. 4 shows four cardinal splines passing through the same points, where the value of the tension is shown for each spline. The appropriate variation range of the tension parameter *t* is from 0.3 to 1 in our experiment.

Another parameter is the weight of the shape constraint α. If α is too big, the segmentation result may become the predefined shape; if it is too small, the segment result may overflow at the weak edges or miss part of the AV because the shape-driven energy has less influence on the surface evolution. According to our experiments, the optimum range of α is between 0.05 and 0.2.

C. Effect of the Shape-driven Energy

In order to evaluate the effect of the shape-driven energy on AV segmentation, two examples are shown in Fig. 5. The AV is partially segmented from the US image in Fig. 5(a), serious overflow occurs in Fig. 5(c), and the AV is segmented successfully in Fig. 5(b) and Fig. 5(d). Consequently, the shape-constrained energy which enlarges the image weak edge force makes the evolution contour approaching object contour more accurately. The selected parameters and corresponding performance of the segmentation results are shown in Table 1. Since the shape-constrained energy drives the evolution contour to approach object contour, the number of iterative of the proposed method is significantly reduced as compared with the original CV model. The execution time of the proposed method has also been significantly reduced. Compared with the CV model, the proposed method is more accurate and efficient.

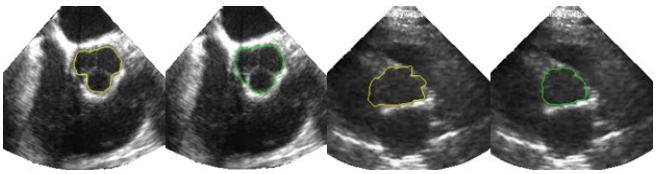

Fig. 5. The illustrations of evolution driven by different energy functions. (a) and (b) show the transesophageal AV B-mode US image, and (c) and (d) show the transthoracic AV B-mode US image; (a) and (c) are acquired by CV model, when (b) and (d) are resulted by the proposed CV model with cardinal shape-driven energy.

TABLE I. PARAMETER AND PERFORMANCE

	Segmentation method	Δ t	α	Iterative Number	Run Time(S)
(a)	CV	0.1	0	65	2.552367
(b)	Proposed	0.1	0.2	20	1.400458
(c)	CV	0.1	0	90	3.076270
(d)	Proposed	0.1	0.05	25	1.830238

D. The Sequence Segmentation Results

Since the sequence of the AV US images are derived from US video format, the position and shape of AV are changed slightly in adjacent frames which have a strong time correlation . Under these circumstances , the segmentation

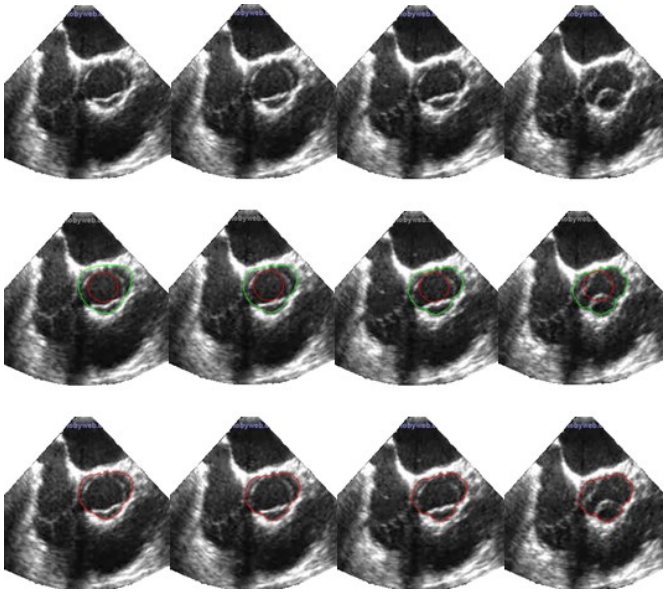

(a) (b) (c) (d)

Fig. 6. The top row shows four consecutive AV US images without segmentation. The mid row indicates the initial contour in red and the outlines of the predefined shape in green. The bottom row indicates the outlines of the AV segmentation results in red.

result of the key frame is served as the predefined shape of the adjacent frames.

As shown in Fig. 6, the initial predefined shape in Fig. 6(a) is constructed by the cardinal spline that passes through the four user defined points. The segmentation result of the previous frame is employed as predefined shape for cases in Fig. 6(b), Fig. 6(c) and Fig. 6(d). In this way, the user interaction is reduced and the efficiency of segmentation can be significantly improved.

E. Assessment

In order to measure the accuracy of the proposed segmentation scheme in AV, the area overlap measure (AOM) [9], average symmetric surface distance (ASD) and maximum symmetric surface distance (MSD) [10] are used to compare our segmentation results with the manual segmentation results of some doctor. To this end, 100 images which consist of 60 transthoracic AV and 40 thransesophageal AV US images are used in this evaluation study. The results of the AV segmentation are shown in Table II. Due to their better AV boundary, the transesophageal datasets has a higher accuracy than the transthoracic datasets. The fact that transthoracic acquisitions are worse than transesophageal images is expected due to the higher frequencies used in transesophageal acquisitions. The result may suggest that the transesophageal US image could be better used for Image Guided Cardiac Intervention.

TABLE II ACCURACY OF AV SEGMENTATION

	AOM (%)	**ASD(mm)**	**MSD(mm)**
60 transthoracic datasets	95.38±2.7	1.4±0.5	2.07±1.3
40 transesophageal datasets	97.21±1.6	0.7±0.15	1.04±0.6

IV. CONCLUSION AND FUTURE WORK

In this paper, a new method has been proposed for segmenting AV from US images, which enhances the CV model with a shape-driven energy functional. One predefined shape is set by radiologist and other predefined shapes can be obtained from the segmented results of the adjacent US frame. Compared with the traditional CV model, the proposed shape-constrained method can segment AV more efficiently and accurately. The performance evaluation of one hundred experimental datasets between the results of the proposed method and the manual segmentation results of doctors demonstrate that the proposed approach is able to produce good result in AV segmentation.

The proposed method is still a semi-automatic method which requires manually defining the initial points. Our future work will be focused on constructing the constrained shape automatically.

ACKNOWLEDGMENT

This work is partially supported by the Chinese NSFC research fund (61190120, 61190124 and 61271318), the Hebei University Biomedical Multidisciplinary Research Center fund (BM201110) and Technological Innovation of Undergraduate research fund (201210075008), the Hebei Province Education Youth Found (Q201223) and Hebei Province Health Research Project (20120399).

REFERENCES

[1] E. J. Howell and J.T.Butcher, "Valvular heart diseases in the developing world: developmental biology takes center stage." J Heart Valve Dis. vol. 21, No.2, March 2012.

[2] J. Alison Noble and Djamal Boukerroui, "US Image Segmentation: A Survey." IEEE Transaction on Medicla Imaging, vol.25, NO.8, Aug. 2006.

[3] Y. Zimmerand, R. Tepper and S. Akselrod, "A two-dimensional extension of minimum cross entropy thresholding for the segmentation of US images," US Med. Biol., 22:1183–1190, 1996.

[4] J.Klingler, J. Vaughan, T. Fraker et al. "Segmentation of echocardiographic images using mathematical morphology." IEEE Trans. on Biomedical Engineering 35, pp. 925–934, 1988.

[5] Y. L. Huang and D. R. Chen, "Watershed segmentation for breast tumor in 2-D sonography," US Med. Biol., vol. 30, no. 5, pp. 625–632, May 2004.

[6] D. Mumford and J. Shah, "Optimal approximation by piecewise smooth functions and associated variational problems," Comm. Pure Appl. Math., 42:577–685 (1989).

[7] T. Chan and L. Vese: Active contours without edges. IEEE Transaction on Image Processing, 10(2):266–277 (2001).

[8] D. Cremers, N. Sochen, and C. Schnorr, "Towards recognition-based variational segmentation using shape priors and dynamic labeling," In L. Griffith, editor, Int. Conf. on Scale Space Theories in Computer Vsion, volume 2695 of LNCS:388–400, Isle of Skye (2003).

[9] B. Sahiner, N. Petrick, H. P. Chan et al. "Computer-aided characterization of mammographic masses: accuracy of mass segmentation and its effects on characterization." IEEE Transactions on medical imaging, VOL. 20, NO. 12, Dec 2001.

[10] T. Heimann, B.Ginneken, M.A.Styner et al. "Comparison and evaluation of methods for liver segmentation from CT datasets," IEEE Transactions on Medical Imaging, VOL. 28, NO. 8, Aug.2009.